Cell Metabolism
Article

# TXNIP Maintains the Hematopoietic Cell Pool by Switching the Function of p53 under Oxidative Stress

Haiyoung Jung,[1,4,8] Mi Jeong Kim,[1,4,8] Dong Oh Kim,[1,4] Won Sam Kim,[1,4] Sung-Jin Yoon,[1,4] Young-Jun Park,[1,4] Suk Ran Yoon,[1,4] Tae-Don Kim,[1,4] Hyun-Woo Suh,[1] Sohyun Yun,[1] Jeong-Ki Min,[1,5] Hee Gu Lee,[2] Young Ho Lee,[6] Hee-Jun Na,[3] Dong Chul Lee,[2] Hyoung-Chin Kim,[7] and Inpyo Choi[1,4,*]
[1]Immunotherapy Research Center
[2]Medical Genomics Research Center
[3]Regenerative Medicine Research Center
Korea Research Institute of Bioscience and Biotechnology, Yuseong-gu, Daejeon 305-806, Republic of Korea
[4]Department of Functional Genomics
[5]Department of Biomolecular Science
University of Science and Technology, Yuseong-gu, Daejeon 305-333, Republic of Korea
[6]Department of Anatomy, School of Medicine, Chungnam National Universtiy, Chung-gu, Daejeon 301-131, Republic of Korea
[7]Biomedical Mouse Resource Center, Korea Research Institute of Bioscience and Biotechnology, Chungbuk 363-883, Republic of Korea
[8]These authors contributed equally to this work
*Correspondence: ipchoi@kribb.re.kr
http://dx.doi.org/10.1016/j.cmet.2013.06.002

## SUMMARY

**Reactive oxygen species (ROS) are critical determinants of the fate of hematopoietic stem cells (HSCs) and hematopoiesis. Thioredoxin-interacting protein (TXNIP), which is induced by oxidative stress, is a known regulator of intracellular ROS. *Txnip*$^{-/-}$ old mice exhibited elevated ROS levels in hematopoietic cells and showed a reduction in hematopoietic cell population. Loss of TXNIP led to a dramatic reduction of mouse survival under oxidative stress. TXNIP directly regulated p53 protein by interfering with p53- mouse double minute 2 (MDM2) interactions and increasing p53 transcriptional activity. *Txnip*$^{-/-}$ mice showed downregulation of the antioxidant genes induced by p53. Introduction of TXNIP or p53 into *Txnip*$^{-/-}$ bone marrow cells rescued the HSC frequency and greatly increased survival in mice following oxidative stress. Overall, these data indicate that TXNIP is a regulator of p53 and plays a pivotal role in the maintenance of the hematopoietic cells by regulating intracellular ROS during oxidative stress.**

## INTRODUCTION

Oxidative stress occurs mainly due to excessive accumulation of cellular reactive oxygen species (ROS) or deficiency of antioxidant defense system. Oxidative stress often leads to pathologic diseases such as diabetes, neurodegenerative diseases, and cancer (Hole et al., 2011; Sinha et al., 2013). There is growing evidence that balanced regulation of ROS is critical for hematopoiesis. Hematopoietic cells are vulnerable to oxidative stress, and malignancy of hematopoietic tissues is observed in the presence of chronic oxidative stress (Ghaffari, 2008). Homeostatic regulation of redox status in hematopoietic tissues is important for normal hematopoiesis.

Thioredoxin-interacting protein (TXNIP) is a 397 amino acid, 50 kDa protein that belongs to the arrestin family, and *Txnip*$^{-/-}$ mice show a high incidence of hepatocellular carcinoma (HCC) (Jeong et al., 2009; Kwon et al., 2011; Lee et al., 2005; Song et al., 2003). TXNIP expression is reduced in many types of tumors, and TXNIP overexpression inhibits tumor growth by blocking cell-cycle progression (Han et al., 2003). The numbers of natural killer (NK) cells in the bone marrow (BM) of *Txnip*$^{-/-}$ mice are reduced, and the long-term reconstituting HSC population shows an exhausted phenotype and is reduced in frequency (Jeong et al., 2009; Lee et al., 2005).

The tumor suppressor p53 plays a key role in restricting the expansion of abnormal cells through either growth arrest or apoptosis in response to genotoxic stresses (Olovnikov et al., 2009; Sablina et al., 2005). The p53 pathway is regulated by mouse double minute 2 (MDM2), an E3 ubiquitin ligase that targets the p53 protein for proteasomal degradation (Sasaki et al., 2011). p53 engages powerful prosurvival pathways by inducing the expression of antiapoptotic or antioxidant genes (Bensaad and Vousden, 2007; Jänicke et al., 2008). In addition, p53 is a critical regulator of HSC quiescence through its target genes (Liu et al., 2009). Previous reports imply that the protective or antiaging effects of TXNIP are important in maintaining hematopoietic cell pool (Jeong et al., 2009; Kim et al., 2007).

In this study, we demonstrate that *Txnip*$^{-/-}$ hematopoietic cells had defects in the regulation of ROS levels and were more sensitive than wild-type cells to oxidative stress. We also demonstrated that TXNIP exerted its antioxidant effects in hematopoietic cells by stabilizing p53 under oxidative stress. Our findings suggest that TXNIP plays a critical role in the antioxidant defense mechanisms of hematopoietic cells by activating the p53 pathway during oxidative stress.

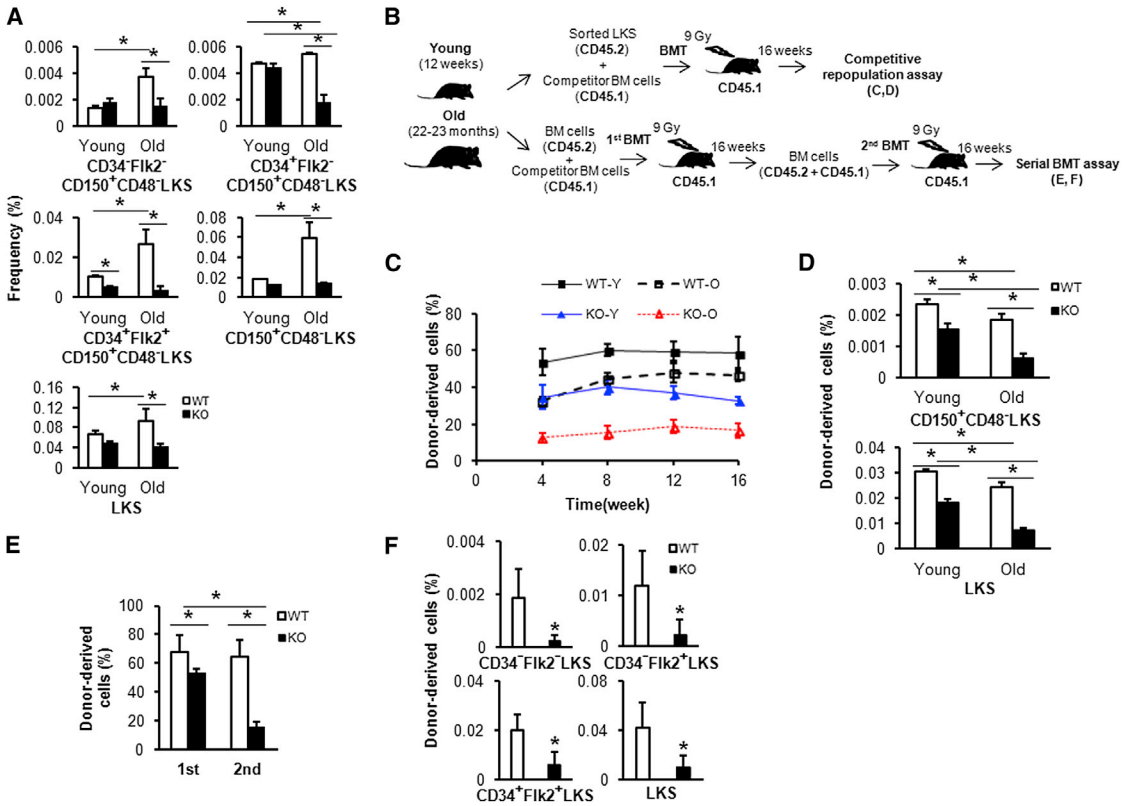


**Figure 1. Defects of Hematopoietic Cell Pool in KO Mice**

(A) Reduced frequencies of HSCs and progenitors in KO mice (n = 4). The frequencies of HSCs and progenitors in young (12 weeks) and old mice (23 months) were analyzed by flow cytometry.

(B) Experimental design for competitive repopulation assays and serial BMT assays.

(C) Decreased donor-derived cell population in old KO mice (n = 5). We transplanted LKS cells ($5 \times 10^3$) from young (12 weeks) and old (23 months) WT or KO mice in combination with competitor cells ($1.0 \times 10^6$) from congenic ($CD45.1^+$) mice into lethally irradiated wild-type (WT) congenic ($CD45.1^+$) recipients.

(D) Distribution of donor-derived HSCs ($CD45.2^+$) among recipient BM cells 16 weeks after transplantation (n = 5).

(E and F) Decreased donor-derived cell population of KO WBM cells after serial transplantation (n = 5). At 16 weeks after the first BMT, we serially injected young donor-derived WBM cells from recipients into a second set of recipient mice (CD45.1). After another 16 weeks, the donor-derived immune cells and frequency of HSCs were examined in the PB (E) and BM (F), respectively. All data are mean ± SD. *$p < 0.05$, **$p < 0.01$. See also Figure S1.

## RESULTS

### Defects of Hematopoietic Cell Maintenance in *Txnip*$^{-/-}$ Mice Are Caused by Elevated ROS

To investigate the effects of TXNIP deficiency on hematopoiesis, we analyzed the frequency of hematopoietic stem cells (HSCs) and hematopoietic progenitors from young (12 weeks) and old (22–23 months) *Txnip*$^{+/+}$ (wild-type [WT]) and *Txnip*$^{-/-}$ (KO) mice. Consistent with previous reports (Geiger and Van Zant, 2002; Sudo et al., 2000), old WT mice showed much higher frequencies of HSCs and hematopoietic progenitors, but old KO mice showed relatively decreased frequencies (Figure 1A). Next, we performed a competitive repopulation assay and a serial bone marrow transplantation (BMT) experiment (Figure 1B). We transplanted lineage$^-$c-Kit$^+$Sca-1$^+$ (LKS) cells or WBM (whole bone marrow) cells from young (12 weeks) and old (22–23 months) mice ($CD45.2^+$) with competitor WBM cells ($CD45.1^+$) into congenic recipients ($CD45.1^+$). Donor-derived cell populations of old WT LKS or WBM cell-transplanted recipients showed little change, but those of old KO LKS or WBM cell-transplanted recipients were markedly decreased (Figure 1C and Figure S1A available online). Also, WBM cells of recipients from young and old KO mice showed a greater reduction in donor-derived cell populations of HSCs and progenitors than those from WT mice (Figures 1D, S1B, and S1C), mostly due to the reduced frequency of HSCs and progenitors in donor WBM or LKS as shown in Figure 1A. Next, we performed a serial BMT experiment. Donor-derived $CD45.2^+$ cells were dramatically decreased in the KO-derived recipient cells (Figures 1E and 1F).

The exhaustion of primitive HSCs is believed to result from increased ROS accumulation following serial transplants, which are a critical determinant of HSC pool maintenance (Abbas et al., 2010; Ito et al., 2006). We found dramatically increased ROS levels in old KO BM cells compared with those from WT littermates (Figure 2A). To assess the effects of the intrinsic increase in ROS on the maintenance of KO BM cells, we transplanted WBM cells ($CD45.2^+$) into lethally irradiated WT congenic ($CD45.1^+$) recipients. After 9 months, we confirmed higher levels of ROS in the KO-derived BM cells (Figure 2B). Our observations

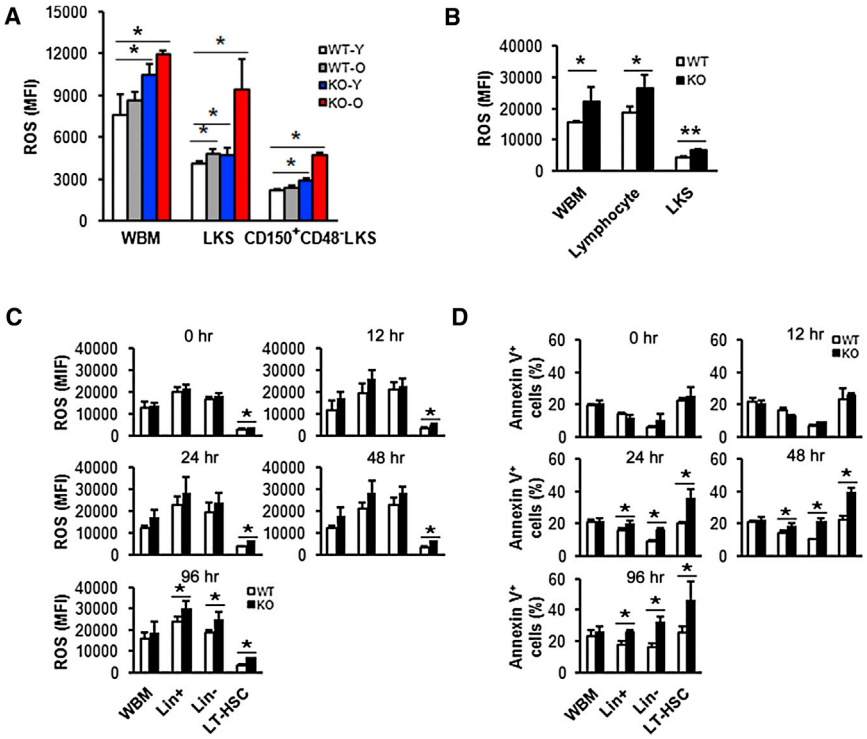


**Figure 2. Regulation of ROS in Hematopoietic Cells by TXNIP under Oxidative Stress**

(A) Elevation of ROS in KO mice (n = 4). ROS levels were measured by DCF staining using flow cytometry from young (12 weeks) and old (23 months) mice.

(B) Elevation of ROS in KO-derived cells after transplantation at 9 months (n = 5). WBM cells ($CD45.2^+$, $2.5 \times 10^6$) from WT or KO mice were noncompetitively transplanted into lethally irradiated WT congenic ($CD45.1^+$) recipients.

(C and D) Time kinetics of ROS (C) and apoptosis (D) of hematopoietic cells after PA (40 mg/kg) challenge. All data are mean ± SD. *$p < 0.05$. See also Figure S2.

suggested that TXNIP plays a critical role in hematopoietic cell antioxidant defense through mechanisms other than its known prooxidant function as an inhibitor of thioredoxin (Trx) (Lee et al., 2005; Patwari et al., 2006; Schulze et al., 2002).

To examine the specificity of antioxidant defense by TXNIP in hematopoietic cells, we analyzed the levels of ROS in WT and KO mouse embryonic fibroblast (MEF) and lung fibroblast cells under oxidative stress. Interestingly, WT MEF and lung fibroblast cells showed the prooxidant function of TXNIP following oxidative stress (Figures S2A–S2D), indicating that TXNIP regulates ROS levels in a cell-type-specific manner. Next, to validate the antioxidant function of TXNIP in hematopoietic cells under oxidative stress, we intraperitoneally (i.p.) injected paraquat (PA), a strong oxidative stress inducer, into young mice. Consistent with our observations of old KO mice, young KO mice showed higher ROS levels and increased cell death in BM cells following PA challenge (Figures 2C and 2D). KO HSCs showed lower ROS levels than nonprimitive cells but also hypersensitivity under oxidative stress. KO HSCs entered into the cell cycle at an early time (0–12 hr) but showed decreased proliferating rates and frequencies at a late time (48–96 hr) following PA challenge (data not shown) (Macip et al., 2003). Taken together, the above data indicate that TXNIP shows cell-type-specific antioxidant function and plays an important role in the maintenance of both HSCs and nonprimitive hematopoietic cells by regulating ROS and cell death following oxidative stress.

## TXNIP Regulates Hematopoietic Cell Maintenance under Oxidative Stress

Next, we tested the effects of oxidative stress on TXNIP-mediated hematopoietic cell maintenance (Figure 3A). PA-pretreated KO BM cells showed a reduction in donor-derived cell populations in recipients (Figures 3B, 3C, S3A, and S3B). PA-challenged KO BM cells also showed decreased colony-forming unit-spleen (CFU-S) numbers (Figure 3D) and a lower survival rate in a radioprotection assay compared to WT (Figure 3E). Overall, these findings suggest that TXNIP maintains the hematopoietic cell pool by regulating ROS levels in vivo following oxidative stress.

## TXNIP Acts as an Antioxidant Protein In Vivo

Based on its roles in hematopoietic cell maintenance, we tested the effects of TXNIP deficiency on the hematopoietic system in terms of protection against oxidative stress in vivo. We challenged mice with 40 mg/kg PA. The KO mice all died within 160 hr, but none of the WT mice died during this time period — they survived more than 2 months. Treatment with N-acetylcysteine (NAC), an antioxidant agent, rescued up to 70% of KO mice (Figure 4A). PA-induced lethality in KO mice was dose and genotype dependent (Figures S4A and S4B). To exclude the possibility of toxic effects on other tissues and to determine the intrinsic response of hematopoietic cells to oxidative stress, we performed BMT experiments. After 8 weeks, we challenged mice with 40 mg/kg PA. All of the mice that received KO WBM cells died within 150 hr, but 70% of the mice that received WT WBM cells survived (Figure 4B). Next, we examined the spleen and thymus following PA challenge. Spleen size and cellularity were markedly decreased in KO mice (Figures 4C, S4C, and S4D). Mice receiving KO WBM also showed a decrease in spleen size following PA challenge (Figure S4E). Similarly, we observed cellular apoptosis in the spleens of PA-treated KO mice with both TUNEL and annexin V staining (Figure 4D). In addition, PA-treated KO mice showed significant damage to the thymus (Figure 4E) and decreased body weight (Figure S4F).

To measure the effects of oxidative stress on host immune defenses, we evaluated lung metastasis. Lung metastasis was markedly increased in PA-challenged KO mice (Figure 4F). PA-challenged KO mice also showed markedly reduced numbers of immune cells associated with tumor cytotoxicity in the spleen

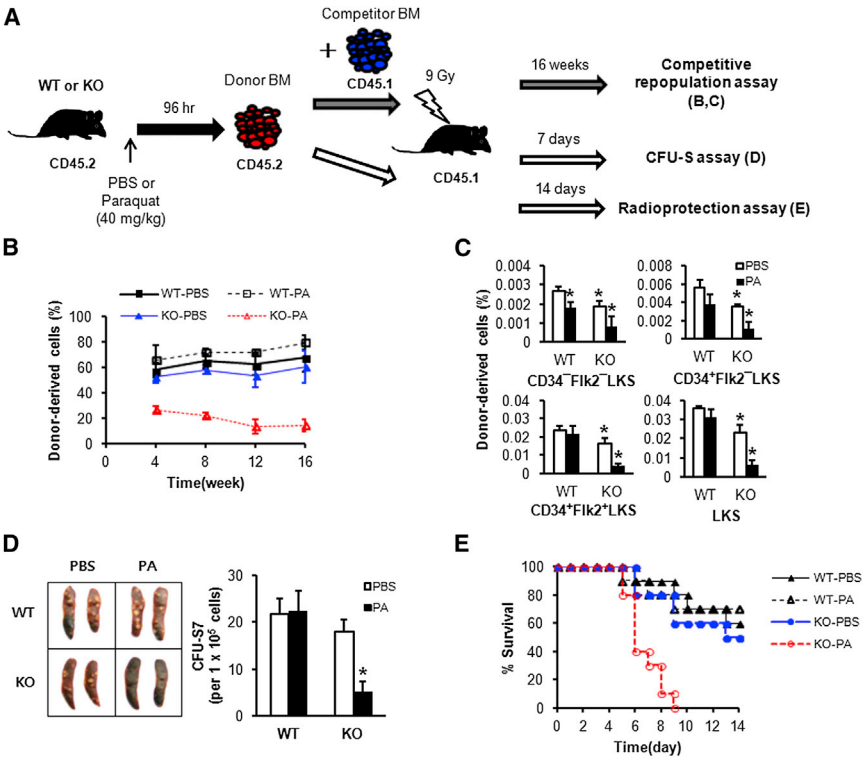


**Figure 3. Loss of Hematopoietic Cell Population in KO Mice Following Oxidative Stress**

(A) Experimental design for competitive repopulation assay, CFU-S assay, and radioprotection assay.

(B) Defects of donor-derived cell population in PA-pretreated KO BM cells (n = 5).

(C) Loss of donor-derived hematopoietic cell population in recipients of BM from PA-pretreated KO mice (n = 5).

(D) Decreased CFU-S numbers in recipients derived from PA-pretreated KO mice (n = 5). After 7 days, the spleens were fixed and the colonies were counted.

(E) Decreased radioprotective function of PA-pretreated KO BM cells (n = 10 per group). The recipient survival was scored and presented as a Kaplan-Meier survival curve. All data are the mean ± SD. *p < 0.05. See also Figure S3.

(Figures S4G–S4I). We further confirmed the immune cell antimetastatic response through BMT. As expected, lung metastasis markedly increased in the mice receiving KO WBM cells, and these mice showed elevated ROS levels of splenocytes (Figures 4G and S4J). Collectively, we found preferential toxic effects of PA on KO immune cells; therefore, KO mice could not maintain functional immune system after PA challenge. These data indicate that TXNIP acts as an antioxidant protein in hematopoietic cells by regulating ROS.

## TXNIP Is Correlated with p53-Mediated ROS Regulation in Hematopoietic Cells

We previously reported that TXNIP expression was highest in long-term (LT)-HSCs and gradually decreased during the progression to short-term (ST)-HSCs and multipotent progenitors (MPPs) (Jeong et al., 2009). To understand the correlation between TXNIP and ROS in BM cells, we examined intracellular ROS and TXNIP levels in BM cells. Interestingly, an inverse correlation was observed between ROS and TXNIP levels in BM cells (Figures 5A and 5B). Recent reports have suggested that the tumor suppressor protein p53 has antioxidant functions and is highly expressed in HSCs. Accordingly, $p53^{-/-}$ mice showed increased ROS levels and dysregulated HSC quiescence (Liu et al., 2008, 2009; Sablina et al., 2005). To evaluate the potential correlation between TXNIP and p53 in BM cells, we measured p53 levels by staining for intracellular p53. The expression of p53 was markedly decreased in KO BM cells (Figure 5C), which was accompanied by higher ROS levels in KO BM cells (Figure 5D). These data strongly suggested a correlation between TXNIP and p53 expression and ROS regulation. Based on the observation of smaller differences in p53 levels and larger differences in ROS levels in KO BM cells compared with those in WT BM cells, it seems that ROS is not entirely regulated by p53 in KO BM cells or is more sensitive to a change of p53 level without TXNIP.

To determine the function of p53 in hematopoietic cells on ROS regulation, we analyzed the levels of ROS in $p53^{-/-}$ hematopoietic cells. $p53^{-/-}$ hematopoietic cells showed higher levels of ROS than WT cells (Figure 5E). To evaluate the double knockdown effect of TXNIP and p53 on ROS regulation in hematopoietic cells, we introduced p53 small hairpin RNA (shRNA) into sorted KO LKS cells in vitro or challenged pifithrin-α (PFT-α), a specific p53 inhibitor, in vivo (Komarov et al., 1999; Liu et al., 2004; Sohn et al., 2009). The effects of shRNAs or PFT-α on p53 and its target gene expression were confirmed (Figures S5A and S5B). The levels of ROS were further increased in $Txnip^{-/-}$ hematopoietic cells by treating p53 shRNA or PFT-α (Figures 5F and 5G). To examine the antioxidant functions of p53 under oxidative stress, we challenged PA into $p53^{-/-}$ mice or PFT-α-pretreated mice. $p53^{-/-}$ hematopoietic cells showed the increased ROS levels following PA challenge (Figures 5H–5J). When PA (50 mg/kg) was injected into WT and $p53^{-/-}$ mice, $p53^{-/-}$ mice were more sensitive to PA challenge (Figure 5K). Furthermore, when PA (40 mg/kg) was injected into WT, $Txnip^{-/-}$, and $Txnip^{-/-}$/PFT-α mice, $Txnip^{-/-}$/PFT-α mice were most sensitive to oxidative stress (Figure 5L). These results strongly suggest that TXNIP works in conjunction with p53 to regulate ROS levels in hematopoietic cells.

## Regulation of p53 Activity by TXNIP via Direct Interaction

p53 and TXNIP were induced and colocalized in the nucleus following $H_2O_2$ treatment in MCF7 (human breast adenocarcinoma) (Figure S6A). These data suggest the possibility of a direct subcellular interaction between TXNIP and p53, so we next examined the interaction between TXNIP and p53. These molecules appeared to directly interact with each other (Figure S6B). Serial mutations of TXNIP followed by glutathione S-transferase

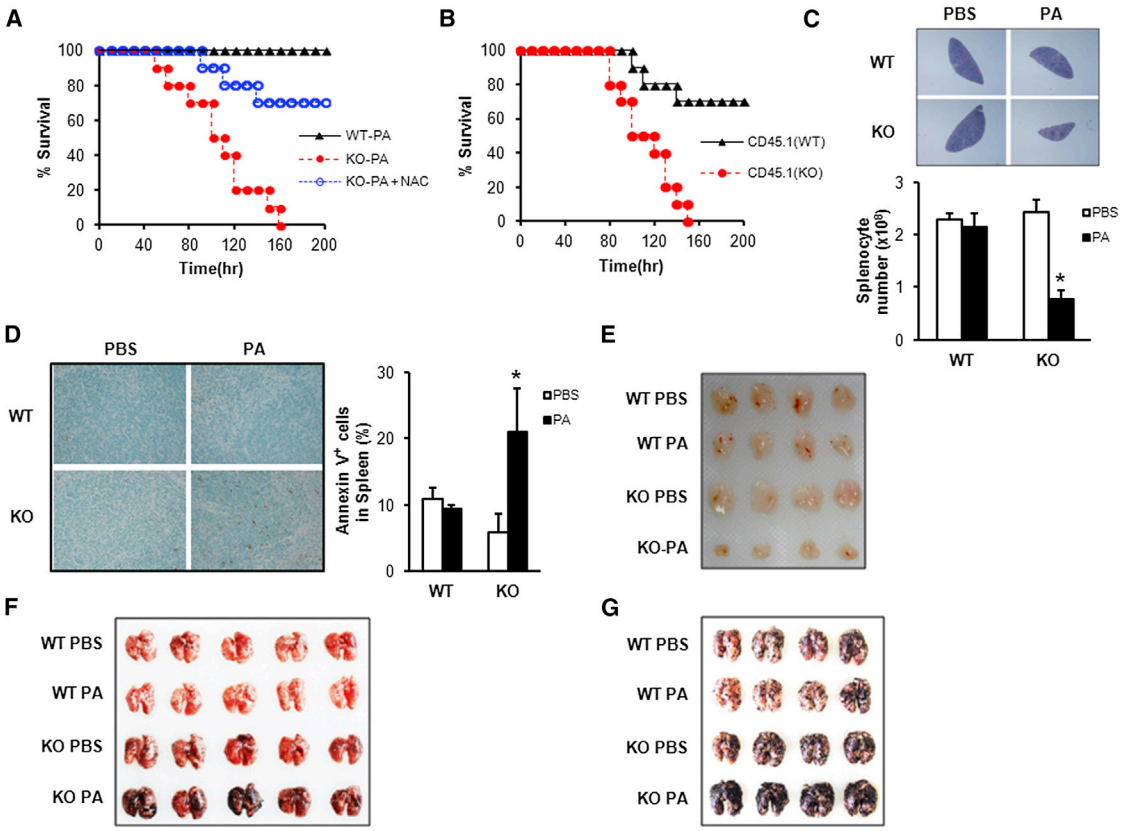


**Figure 4. TXNIP Regulates the Homeostasis of the Immune System under Oxidative Stress**

(A) Mice survival assay. WT or KO mice were challenged with PA (40 mg/kg). For NAC rescue, we injected 100 mg/kg NAC daily starting at day −1. Mice survival is presented as a Kaplan-Meier survival curve (n = 10 per group).

(B) Mice survival assay after BMT (n = 10 per group). WBM cells ($CD45.2^+$, $2.5 \times 10^6$) from WT and KO mice were injected into lethally irradiated WT congenic ($CD45.1^+$) recipients. After 8 weeks, assays were performed using the same methods as described in (A).

(C) Hematoxylin and eosin (H&E) stained images (400×) and spleen cellularity (n = 5). WT or KO mice were challenged with PA (40 mg/kg) for 96 hr.

(D) Apoptosis of splenocytes (n = 5). Spleens were stained with TUNEL or annexin V for the apoptosis assay. Representative images of TUNEL-stained spleen (left, 400×) and annexin V splenocytes are shown.

(E) Thymus damage following oxidative stress (n = 4). WT or KO mice were challenged with PA (40 mg/kg) for 96 hr.

(F) Lung metastasis induced in KO mice by oxidative stress (n = 5).

(G) Induced lung metastasis in KO-derived recipients after BMT. These experiments were independently repeated twice. The results are shown as a representative photograph of metastatic nodules on the lungs (n = 4). All data are mean ± SD. *$p < 0.05$. See also Figure S4.

(GST) pull-downs revealed that two cysteine residues (247 and 267) of TXNIP were critical for their interaction (Figure 6A) (Shin et al., 2008). To determine the p53 residues necessary for this interaction, we generated two deletion mutants by deleting either the N-terminal or C-terminal DNA-binding domain (DBD) of the p53. TXNIP interacted with the C-terminal DBD region of p53, which contains five cysteines (Figure 6B). Interactions between TXNIP and p53 were increased, but TXNIP dissociated from Trx following $H_2O_2$ treatment (Figure 6C). Furthermore, to determine the status of the Trx-Trx reductase system in *Txnip*$^{-/-}$ hematopoietic cells, we examined the level of Trx and measured the enzyme activity. The expression and reducing activity of Trx was not changed in KO LKS or lineage$^-$c-Kit$^+$ (LK) cells but significantly increased in KO lung fibroblasts (Figures S6C–S6F). These results suggest cell-type-specific regulation of Trx by TXNIP.

Next, we investigated the interaction between TXNIP and p53 by redox stress. The dithiothreitol (DTT)-treated TXNIP showed decreased coprecipitation with p53, which was not altered following $H_2O_2$ treatment in vitro (Figure S6G) (Jung et al., 2008). We also examined the oxidation of TXNIP under acute oxidative stress. Redox blot showed the oxidized TXNIP following $H_2O_2$ treatment (Figure S6H). To investigate the physiological consequences of the interaction between TXNIP and p53, we examined the cellular levels of p53 in TXNIP (WT) or TXNIP (C247S/C267S [DM])-overexpressing cells. Cellular levels of p53 were increased by TXNIP (WT) expression, but not by TXNIP (DM) in Baf3 cells (murine bone marrow-derived pro-B cells) (Figure 6D). To determine whether the increase of p53 was dependent on its protein level, we examined the level of p53 transcripts in *Txnip*$^{-/-}$ cells. RT-PCR revealed no significant changes of p53 messenger RNA (mRNA) expression in the absence of TXNIP (Figure S6I).

Next, we investigated the effects of TXNIP or TXNIP-small interacting RNA (siRNA) on p53 stability. p53 levels were retained in TXNIP overexpressing cells, but TXNIP-siRNA

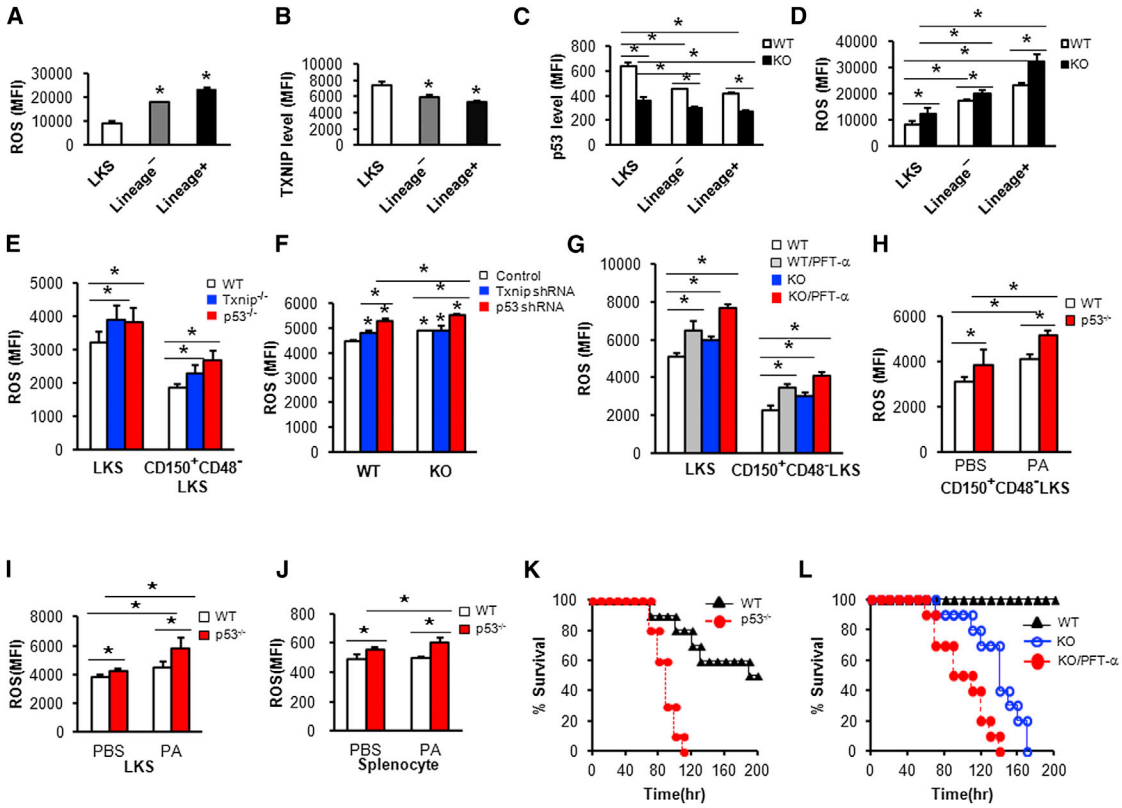


**Figure 5. Inverse Correlation between TXNIP and p53 Expression and ROS in BM Cells**

(A) ROS levels in WT BM cells (n = 3). ROS levels were measured by the DCFDA assay using flow cytometry.

(B and C) Intracellular staining for TXNIP (B) and p53 (C) in WT or KO BM cells (n = 3). BM cells were stained with surface markers and anti-TXNIP or -p53 antibodies.

(D) ROS levels in WT and KO BM cells (n = 4).

(E) Elevation of ROS in *Txnip*$^{-/-}$ and *p53*$^{-/-}$ HSCs and LKS cells (n = 3).

(F) Increased ROS levels in LKS cells from WT and KO mice by TXNIP shRNA or p53 shRNA introduction (n = 3). We introduced TXNIP shRNA and p53 shRNA into LKS cells 3 times for 3 days in vitro. These experiments were independently repeated 2 times.

(G) Elevation of ROS in WT and KO HSCs following p53 inhibitor (PFT-α) treatment (n = 4). We injected PFT-α (5 mg/kg) into WT or KO mice. After 48 hr, mice were killed, and we analyzed their ROS levels of BM cells.

(H–J) Increased ROS in *p53*$^{-/-}$ hematopoietic cells after PA challenge (n = 3). WT and *p53*$^{-/-}$ mice were treated with PA (40 mg/kg) for 24 hr. (H) Increased ROS in *p53*$^{-/-}$ CD150$^{+}$CD48$^{-}$LKS cells. (I) Increased ROS in *p53*$^{-/-}$ LKS cells. (J) Increased ROS in *p53*$^{-/-}$ splenocytes.

(K) Mice survival assay (n = 10 per group). WT or *p53*$^{-/-}$ mice were challenged with PA (50 mg/kg). Mice survival was scored every 12 hr and presented as a Kaplan-Meier survival curve.

(L) Mice survival assay (n = 10 per group). We injected PFT-α (5 mg/kg) into KO mice 24 hr before PA injection and then injected PA (40 mg/kg) into WT, KO, and KO/PFT-α mice. All data are mean ± SD. *p < 0.05. See also Figure S5.

reduced p53 stability (Figure S6J). The stability of p53 is tightly regulated by MDM2, an E3 ubiquitin ligase, via ubiquitination-dependent proteasomal degradation (Sasaki et al., 2011). Therefore, we examined the effects of TXNIP on p53-MDM2 interactions. TXNIP significantly decreased the association between p53 and MDM2 (Figures 6E and S6K). Consistently, p53 ubiquitination was markedly decreased in TXNIP-overexpressing cells (Figure S6L). Furthermore, the physical interaction between TXNIP and p53 also markedly increased p53-mediated transcriptional activity in cells (Figure 6F). Collectively, these results indicate that TXNIP increased p53 stability by interfering with the interactions between p53 and MDM2, thereby inducing the transcriptional activity of p53.

## TXNIP Mediates the Antioxidant Effect of p53 In Vivo

The above results strongly suggested the possibility that TXNIP regulated the antioxidant activity of p53 through the expression of p53-dependent antioxidant genes. WT LKS cells showed higher expression of p53 and its target genes, *SESN1* and *SESN2* (Figure 7A), and similar expression of p53 target genes was observed in WT LK cells by western blot (Figure 7B). Next, we showed differential expression of p53 target antioxidant genes in WT and KO LKS cells (Figure 7C). Interestingly, stronger induction of p53 target prooxidant genes was observed in KO LKS cells at 24 hr under oxidative stress (Figure 7D), which might correlate with p53 activation by excessively elevated ROS levels (Figures 2C and S7A), similar to that observed in old KO mice (Figure 2A). The expression of TXNIP was increased, and

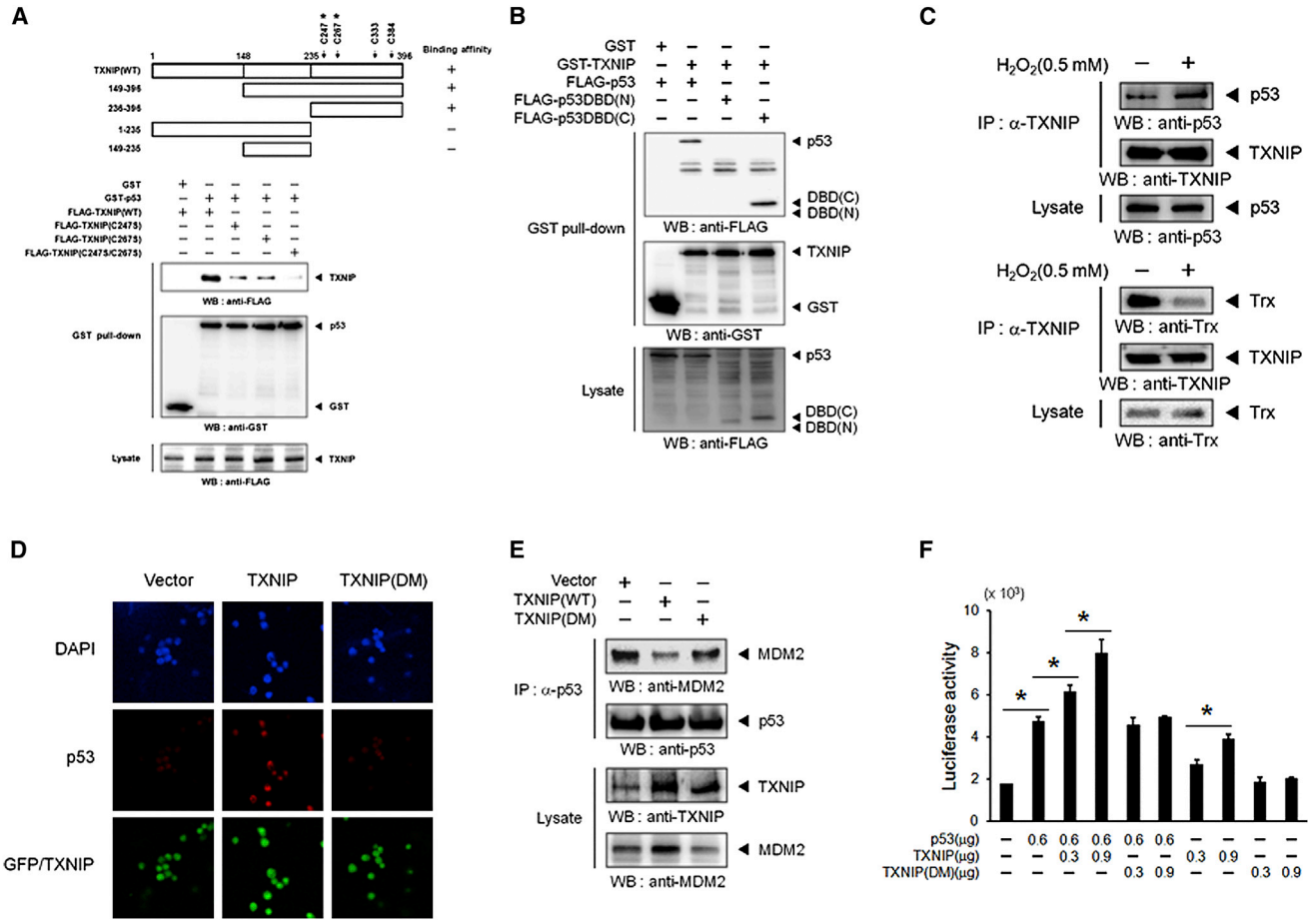


**Figure 6. TXNIP Interacts with p53 and Regulates its Transcriptional Activity**

(A) TXNIP interacts with p53 via its cysteine residues C247 and C267. We cotransfected p53- and TXNIP-encoding vectors into 293T cells. The protein complexes were analyzed using GST pull-down assay as described previously (Jung et al., 2008; Shin et al., 2008).

(B) p53 interacts with TXNIP via its C-terminal DBD.

(C) Interaction of TXNIP with p53 or Trx following $H_2O_2$ treatment. Baf3 cells were treated with $H_2O_2$ (0.5 mM) for 6 hr. Cell lysates were immunoprecipitated with TXNIP antibodies.

(D) Induction of p53 by TXNIP overexpression. Baf3 cells were transiently transfected with pMYs-IRES-GFP vector, pMYs-IRES-GFP-mTXNIP, or pMYs-IRES-GFP-mTXNIP (DM). The cells were immunostained with anti-p53 and then analyzed by confocal microscopy.

(E) Regulation of the p53-MDM2 complex by TXNIP expression. pMYs-IRES-GFP vector, pMYs-IRES-GFP-mTXNIP, or pMYs-IRES-GFP-mTXNIP(DM) was transfected into Baf3 cells, and interaction was determined by immunoprecipitation with anti-p53 antibody.

(F) Induction of the transcriptional activity of p53 by TXNIP. Baf3 cells were transfected with increasing amounts of TXNIP or TXNIP (DM), as indicated, along with p53-luciferase reporter and pRL-CMV plasmid vectors. All of the experiments were independently repeated at least three times, and data are mean ± SD. *p < 0.05. See also Figure S6.

differential kinetics of p53 activation was observed under oxidative stress in lineage$^-$ cells (Figure 7E). Additionally, we found higher levels of p53 and its target genes accompanied by elevated apoptosis and cell-cycle arrest in old KO mice, suggesting that p53 was activated by the elevated ROS levels in old KO mice (Figures S7B–S7D).

Next, to provide direct evidence that the p53 antioxidant function was regulated by interactions with TXNIP in vivo, we introduced TXNIP(WT), TXNIP(DM), or p53 into KO BM cells and then transplanted them into lethally irradiated WT congenic (CD45.1$^+$) recipients. Expression of TXNIP(WT), TXNIP(DM), or p53 in KO BM cells was confirmed by real-time PCR (Figure S7E). After 8 weeks, mice were challenged with 40 mg/kg PA and were examined for changes in the frequency of HSCs and progenitors and mice survival. Introduction of TXNIP(WT) or p53 rescued the frequencies of KO donor (CD45.2) hematopoietic cells and showed higher survival rates, but the TXNIP(DM) mutant did not (Figures 7F and 7G). Thus, our results provided direct evidence that the antioxidant effect of TXNIP was mediated by interactions with the p53 pathway in vivo.

## DISCUSSION

Oxidative stress basically defines a condition in which the prooxidant-antioxidant balance in the cell is disturbed. In hematopoietic cells, the defects of antioxidant pathways can lead to oxidative stress and deficiencies in several ROS scavengers, resulting in anemia and malignancies of hematopoietic tissues

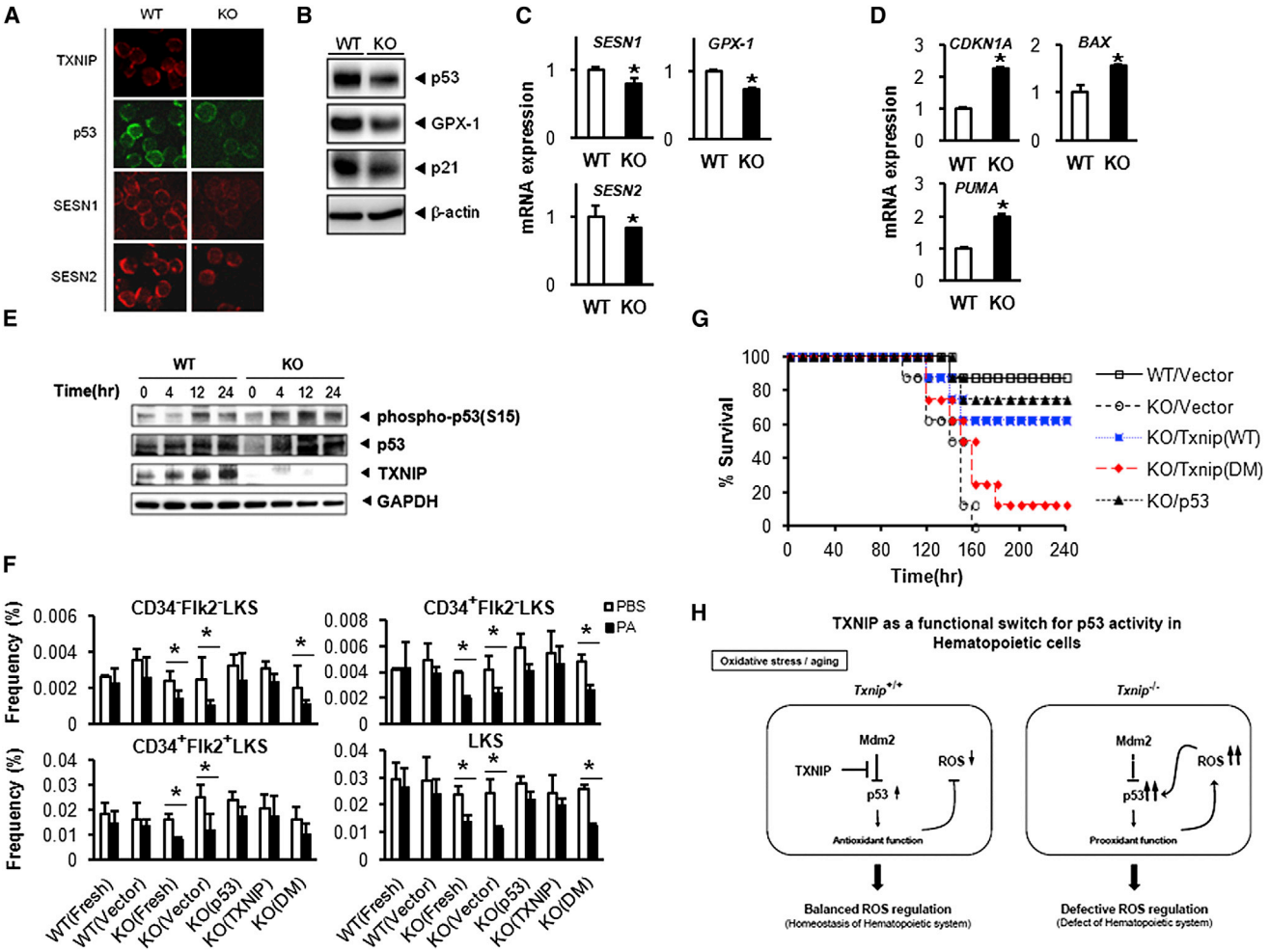


**Figure 7. TXNIP Regulates the Antioxidant Effect of p53 in Hematopoietic Cells**

(A) Intracellular staining of p53 target genes in LKS cells.

(B) Expression of p53 target genes in lineage$^-$c-Kit$^+$ (LK) cells.

(C) Regulation of p53 target antioxidant genes in WT and KO LKS cells.

(D) Regulation of p53 target prooxidant genes in WT and KO LKS cells after PA challenge. WT and KO mice were challenged with PA (40 mg/kg) for 24 hr, and p53 target genes were evaluated by quantitative real-time PCR.

(E) Time kinetics of p53 expression in WT and KO lineage$^-$ BM cells following PA (40 mg/kg) treatment.

(F) Rescue of HSCs and progenitors from oxidative stress by introducing TXNIP and p53 genes into KO BM cells (n = 4 or 5 per group). After 8 weeks, the recipients were challenged with PA (40 mg/kg) for 96 hr.

(G) Rescue of mice survival by introducing TXNIP and p53 into KO BM cells. Transplanted recipients were challenged with PA (40 mg/kg), and mouse survival was presented as a Kaplan-Meier survival curve (n = 8 per group).

(H) TXNIP acts as a functional switch to determine the cellular function of p53 in hematopoietic cells in response to oxidative stress. TXNIP can regulate the context of hematopoietic cells by regulating the activity of p53 under oxidative stress. WT hematopoietic cells are ready to defend ROS stress by inducing the p53 target antioxidant genes, but KO hematopoietic cells are damaged by elevated ROS, resulting from the reduction of antioxidant genes expression. All data are mean ± SD. *$p < 0.05$. See also Figure S7.

(Ghaffari, 2008; Sinha et al., 2013). Thus, the excessive oxidative stress impairs hematopoietic cell functions and leads to abnormal hematopoiesis.

We first showed that ROS levels were elevated in TXNIP KO hematopoietic cells and determined that elevated ROS levels induced hematopoietic cell apoptosis in *Txnip*$^{-/-}$ mice and impaired their subsequent hematopoiesis, consistent with previous reports (Blank et al., 2008; Naka et al., 2008). Accumulating research indicates the importance of ROS in hematopoietic cells and that levels can become elevated following the loss of functional genes (Ito et al., 2004; Miyamoto et al., 2007). In this study, we observed an antioxidant effect of TXNIP in hematopoietic cells undergoing oxidative stress. TXNIP is also a candidate tumor suppressor, and its expression is dramatically reduced in various tumor tissues (Kwon et al., 2010). Tumor cells have high levels of ROS, and TXNIP protein levels are markedly decreased in renal cell carcinoma (Dutta et al., 2005; Gupta et al., 1999). Meanwhile, the prooxidant function of TXNIP was observed in nonhematopoietic cells, such as MEFs and lung fibroblast cells, following oxidative stress. Collectively, these

results indicate that the amount of TXNIP is inversely associated with the ROS level in hematopoietic cells, and the loss of TXNIP can increase ROS levels in a cell-type-specific manner.

p53 can protect cells against genotoxic damage by inducing antiapoptotic and antioxidant genes (Bensaad and Vousden, 2007; Han et al., 2008; Jänicke et al., 2008). Increased levels of alternative reading frame protein of the *Cdkn2a* locus (ARF) and p53 have been shown to decrease ROS levels in splenocytes and increase their resistance to acute oxidative stress following PA challenge (Matheu et al., 2007). $p53^{-/-}$ mice show increased levels of oxidation markers in tissue and hypersensitivity to lipopolysaccharide (LPS)-induced septic shock (Komarova et al., 2005). TXNIP and p53 appear to be involved in overlapping aspects of cellular functions, including tumor suppression, cell-cycle arrest, ROS regulation, and hematopoietic cell maintenance, strongly suggesting that they cooperate to regulate ROS levels in hematopoietic cells.

Here, we show that TXNIP interacts directly with p53 via cysteine residues and increases p53 stability by inhibiting the formation of the p53-MDM2 complex, thereby inducing the transcriptional activity of p53. TXNIP also directly interacts with Trx and inhibits interactions between Trx and other factors, such as ASK-1 and PAG (Kim et al., 2007). TXNIP links oxidative stress to inflammasome activation by interacting with NLRP3, and inflammasome activators induce the dissociation of TXNIP from Trx in a ROS-sensitive manner (Zhou et al., 2010). We also found that TXNIP was dissociated from Trx by oxidative stress. However, the interaction between TXNIP and p53 was increased by oxidative stress. We recently reported that the association of TXNIP with HDAC1 and HDAC3 via the cysteine 247 residue resulted in the suppression of NF-κB activity (Kwon et al., 2010). A recent report suggested that TXNIP-infected human embryonic lung diploid fibroblast 2BS cells showed an induction of p53 and p21 during cellular senescence (Zhuo et al., 2010). The above reports provided a clue as to how p53 may be regulated by TXNIP. The tumor suppressor p53 contains ten cysteine residues in its DNA-binding domain, and the reduction of cysteine residues leads to enhanced binding, whereas oxidation abolishes binding (Hainaut and Milner, 1993; Hupp et al., 1993; Rainwater et al., 1995). Several proteins have been reported to inhibit p53-MDM2 interactions through direct binding to p53 or MDM2 (Hsieh et al., 1999; Jung et al., 2007; Leung et al., 2002). For example, NM23-H1 and STRAP (serine-threonine kinase receptor-associated protein) interact with the DNA-binding domain of p53 via cysteine residues and activate p53 activity by interfering with the p53-MDM2 complex. ARF, the alternative reading frame product of the INK4a/ARF locus, binds MDM2 and prevents MDM2-mediated p53 degradation (Jung et al., 2008).

p53 can also activate an antioxidant transcriptional program that could be relevant when p53 is activated by mild stresses (Vousden and Lane, 2007). We showed the differential expression of p53 target genes in WT and KO cells, suggesting that the induction of the p53 response program could be regulated by TXNIP. Reduction of the antioxidant genes in KO hematopoietic cells might lead to an imbalance in the intracellular defense system, and KO hematopoietic cells showed elevated ROS levels and became more sensitive to oxidative stress. We detected higher levels of p53 and its target genes in old KO BM cells due to hyperphysiological ROS levels, which led to apoptosis and cell-cycle arrest. p53 exerts different effects on cellular redox status by directly regulating the expression of prooxidant or antioxidant genes, depending on the strength of the oxidative stress (Liu et al., 2005; Sablina et al., 2005; Stambolsky et al., 2006). However, the key regulatory molecule responsible for switching p53 function from antioxidant to prooxidant in response to different levels of oxidative stress has not yet been discovered. In this study, we observed that p53 functions as an antioxidant in WT BM cells, but it could also function as a prooxidant in KO BM cells with elevated ROS. Therefore, we propose that TXNIP acts as a functional switch to determine the cellular function of p53 in hematopoietic cells in response to oxidative stress (Figure 7H).

In conclusion, we found that TXNIP plays important roles in the maintenance of the hematopoietic cells by regulating the p53 pathway. KO mice showed reduced hematopoietic cell population, impaired hematopoietic cell maintenance, and increased apoptosis following oxidative stress, leading to death after PA challenge. Restoring TXNIP and p53 expression rescued hematopoietic cell pool and mice survival under oxidative stress. These results suggest that modulating TXNIP and p53 interactions could potentially be a therapeutic target for oxidative stress-related diseases such as hematopoietic malignancies and metabolic diseases.

## EXPERIMENTAL PROCEDURES

### Mice Experiments

TXNIP KO mice were generated as described previously (Lee et al., 2005), and congenic CD45.1$^+$ C57BL/6 mice and $p53^{-/-}$ mice (B6.129S2-Trp53$^{tm1Tyj}$/J) were purchased from Jackson Laboratory. All mice were housed in a pathogen-free animal facility under a 12 hr light-dark cycle, and we used young (8–12 weeks) and old (22–23 months) male mice. $p53^{-/-}$, $Txnip^{-/-}$ (KO), and WT mice were injected i.p. with 40, 50, or 80 mg/kg PA and 100 mg/kg NAC (Sigma-Aldrich) or 5 mg/kg PFT-α (Sigma-Aldrich). All experiments were performed in compliance with the *Guide for the Care and Use of Laboratory Animals*, from the Institute for Laboratory Animal Research.

### Preparation of BM Cells

Total BM cells were isolated from mouse femurs, tibias, hip bones, and shoulder bones by grinding tissues in RPMI 1640 medium (WelGENE) plus 2% fetal bovine serum (FBS). Red blood cells (RBCs) were lysed using ACK buffer (0.15 M $NH_4Cl$, 1.0 mM $KHCO_3$, 0.1 mM EDTA [pH 7.4]) or not, and the cells were filtered through a strainer. Antibodies were purchased from BD Biosciences or BioLegend. BM cells were stained as previously described (Jeong et al., 2009) and analyzed using FACSCanto II, and LKS cells were sorted using FACSAria Cell Sorter (BD Biosciences). For lineage$^-$c-Kit$^+$ (LK) cell preparation, we used magnetic-activated cell sorting (MACS) purification methods.

### Bone Marrow Transplantation

For competitive repopulation assays, WBM cells ($2.0 \times 10^6$) or LKS cells ($5.0 \times 10^3$) from young and old WT or KO mice (CD45.2$^+$) and from congenic (CD45.1$^+$, $1.0 \times 10^6$) mice were mixed, and the mixture was intravenously (i.v.) injected into lethally irradiated (9 Gy) WT congenic (CD45.1$^+$) recipients. The repopulation of donor-derived cells was monitored by staining peripheral blood cells (PB) obtained from tail vein and BM cells with antibodies against indicated surface markers. For noncompetitive transplantation, WBM cells ($2.5 \times 10^6$) from WT or KO mice were i.v. injected into lethally irradiated (9 Gy) WT congenic (CD45.1$^+$) recipients and assayed after 8 weeks.

### Detection of Intracellular ROS

Intracellular levels of ROS were measured by flow cytometry using the ROS-specific fluorescent probes 5-(and 6)-chloromethyl-2′,7′-dichlorodihydrofluorescein diacetate, acetyl ester (DCF) (C6827) and dihydroethidium (DHE)

(D11347) (Invitrogen). Freshly isolated cells were incubated for 15 min at 37°C at a final concentration of 5 μM DCF or 2.5 μM DHE in PBS containing 2% FBS.

### CFU-S and Radioprotection Assay

Lethally irradiated (9 Gy) WT congenic (CD45.1$^+$) recipients were i.v. injected with BM cells (1 × $10^5$) from PBS or PA-treated WT and KO mice and spleens were fixed in Carnoy's solution (60% ethanol, 30% chloroform, 10% acetic acid [v/v]), and macroscopic colonies were counted after 7 days. For radioprotection assay, we adjusted the number of WT BM cells to keep a survival rate of more than 60% after BMT. RBCs were lysed in donor WBM cells, and 1.5 × $10^5$ BM cells from WT PBS, WT PA, KO PBS, or KO PA were injected into lethally irradiated (9 Gy) congenic (CD45.1$^+$) recipients. These results might explain that the mice that received enough number of HSCs from donor BM cells could survive after BMT due to normal hematopoiesis. The recipient survival was scored every day and presented as a Kaplan-Meier survival curve.

### Cell Culture and Reporter Assay

A549, MCF7, HCT116 (+/+, −/−), and 293T cells were cultured in Dulbecco's modified Eagle's medium (DMEM) or RPMI 1640 medium supplemented with 10% FBS (HyClone). Baf3 (murine bone marrow-derived pro-B cell) cells were cultured in RPMI 1640 medium supplemented with 10% FBS and 10 ng/ml mouse interleukin-3 (IL-3). Lung fibroblast cells were isolated from WT or KO mice as described previously (Huaux et al., 2003) and cultured in DMEM supplemented with 10% FBS (we used 1–2 passages). MEF cells were prepared from day 13.5 embryos, and we used 1–3 passages. Each construct was transiently transfected with Lipofectamine and Plus (Invitrogen) or Amaxa Cell Line Nucleofector Kit V (Lonza) according to the manufacturer's instructions. Luciferase activity was monitored by using a p53-luciferase reporter (Jung et al., 2008), and *Renilla* luciferase expression vector (Promega) was cotransfected as a control to monitor the transfection efficiency. The firefly and *Renilla* luciferase activities were determined using the Dual-Luciferase Reporter Assay System (Promega) (Jeong et al., 2009).

### Statistical Analyses

The data are expressed as the mean ± SD of n determinations unless noted otherwise, and Student's t test was used to compare two groups. $p < 0.05$ was considered statistically significant.

## SUPPLEMENTAL INFORMATION

Supplemental Information includes Supplemental Experimental Procedures and seven figures and can be found with this article online at http://dx.doi.org/10.1016/j.cmet.2013.06.002.

## ACKNOWLEDGMENTS

This work was supported in part by grants from the GRL project and the New Drug Target Discovery Project (M10848000352-08N4800-35210), the Ministry of Education, Science & Technology, the Korean Health Technology R&D Project (A121934), Ministry of Health and Welfare, STP Project (DTM0241111) from Ministry of Knowledge Economy, and KRIBB Research Initiative Program, Republic of Korea. We would like to thank Hyang Ran Yoon (Medical Genomics Research Center, KRIBB) for experimental help. We would like to thank Dr. Shinya Yamanaka (Kyoto University, Japan) for providing the pMXs-p53 clone.

H.J. designed and performed all experiments, analyzed the data, and wrote the manuscript. M.J.K. performed experiments and analyzed the data. D.O.K., W.S.K., and S.-J.Y. performed experiments. Y.H.L. performed immunohistochemistry of spleens. Y.-J.P., S.R.Y., T.-D.K., J.-K.M., H.G.L., H.-J.N., D.C.L., and S.Y. provided helpful discussions and crucial analysis of data. H.-W.S. constructed TXNIP mutants. H.-C.K. provided *p53*$^{-/-}$ mice and helpful discussions. I.C. supervised the overall project, analyzed the data, and wrote the manuscript. The authors declare no competing financial interests.

Received: April 12, 2012
Revised: December 12, 2012
Accepted: May 31, 2013
Published: July 2, 2013

## REFERENCES

Abbas, H.A., Maccio, D.R., Coskun, S., Jackson, J.G., Hazen, A.L., Sills, T.M., You, M.J., Hirschi, K.K., and Lozano, G. (2010). Mdm2 is required for survival of hematopoietic stem cells/progenitors via dampening of ROS-induced p53 activity. Cell Stem Cell *7*, 606–617.

Bensaad, K., and Vousden, K.H. (2007). p53: new roles in metabolism. Trends Cell Biol. *17*, 286–291.

Blank, U., Karlsson, G., and Karlsson, S. (2008). Signaling pathways governing stem-cell fate. Blood *111*, 492–503.

Dutta, K.K., Nishinaka, Y., Masutani, H., Akatsuka, S., Aung, T.T., Shirase, T., Lee, W.H., Yamada, Y., Hiai, H., Yodoi, J., and Toyokuni, S. (2005). Two distinct mechanisms for loss of thioredoxin-binding protein-2 in oxidative stress-induced renal carcinogenesis. Lab. Invest. *85*, 798–807.

Geiger, H., and Van Zant, G. (2002). The aging of lympho-hematopoietic stem cells. Nat. Immunol. *3*, 329–333.

Ghaffari, S. (2008). Oxidative stress in the regulation of normal and neoplastic hematopoiesis. Antioxid. Redox Signal. *10*, 1923–1940.

Gupta, A., Rosenberger, S.F., and Bowden, G.T. (1999). Increased ROS levels contribute to elevated transcription factor and MAP kinase activities in malignantly progressed mouse keratinocyte cell lines. Carcinogenesis *20*, 2063–2073.

Hainaut, P., and Milner, J. (1993). Redox modulation of p53 conformation and sequence-specific DNA binding in vitro. Cancer Res. *53*, 4469–4473.

Han, S.H., Jeon, J.H., Ju, H.R., Jung, U., Kim, K.Y., Yoo, H.S., Lee, Y.H., Song, K.S., Hwang, H.M., Na, Y.S., et al. (2003). VDUP1 upregulated by TGF-beta1 and 1,25-dihydorxyvitamin D3 inhibits tumor cell growth by blocking cell-cycle progression. Oncogene *22*, 4035–4046.

Han, E.S., Muller, F.L., Pérez, V.I., Qi, W., Liang, H., Xi, L., Fu, C., Doyle, E., Hickey, M., Cornell, J., et al. (2008). The in vivo gene expression signature of oxidative stress. Physiol. Genomics *34*, 112–126.

Hole, P.S., Darley, R.L., and Tonks, A. (2011). Do reactive oxygen species play a role in myeloid leukemias? Blood *117*, 5816–5826.

Hsieh, J.K., Chan, F.S., O'Connor, D.J., Mittnacht, S., Zhong, S., and Lu, X. (1999). RB regulates the stability and the apoptotic function of p53 via MDM2. Mol. Cell *3*, 181–193.

Huaux, F., Liu, T., McGarry, B., Ullenbruch, M., and Phan, S.H. (2003). Dual roles of IL-4 in lung injury and fibrosis. J. Immunol. *170*, 2083–2092.

Hupp, T.R., Meek, D.W., Midgley, C.A., and Lane, D.P. (1993). Activation of the cryptic DNA binding function of mutant forms of p53. Nucleic Acids Res. *21*, 3167–3174.

Ito, K., Hirao, A., Arai, F., Matsuoka, S., Takubo, K., Hamaguchi, I., Nomiyama, K., Hosokawa, K., Sakurada, K., Nakagata, N., et al. (2004). Regulation of oxidative stress by ATM is required for self-renewal of haematopoietic stem cells. Nature *431*, 997–1002.

Ito, K., Hirao, A., Arai, F., Takubo, K., Matsuoka, S., Miyamoto, K., Ohmura, M., Naka, K., Hosokawa, K., Ikeda, Y., and Suda, T. (2006). Reactive oxygen species act through p38 MAPK to limit the lifespan of hematopoietic stem cells. Nat. Med. *12*, 446–451.

Jänicke, R.U., Sohn, D., and Schulze-Osthoff, K. (2008). The dark side of a tumor suppressor: anti-apoptotic p53. Cell Death Differ. *15*, 959–976.

Jeong, M., Piao, Z.H., Kim, M.S., Lee, S.H., Yun, S., Sun, H.N., Yoon, S.R., Chung, J.W., Kim, T.D., Jeon, J.H., et al. (2009). Thioredoxin-interacting protein regulates hematopoietic stem cell quiescence and mobilization under stress conditions. J. Immunol. *183*, 2495–2505.

Jung, H., Seong, H.A., and Ha, H. (2007). NM23-H1 tumor suppressor and its interacting partner STRAP activate p53 function. J. Biol. Chem. *282*, 35293–35307.

Jung, H., Seong, H.A., and Ha, H. (2008). Critical role of cysteine residue 81 of macrophage migration inhibitory factor (MIF) in MIF-induced inhibition of p53 activity. J. Biol. Chem. *283*, 20383–20396.

Kim, S.Y., Suh, H.W., Chung, J.W., Yoon, S.R., and Choi, I. (2007). Diverse functions of VDUP1 in cell proliferation, differentiation, and diseases. Cell. Mol. Immunol. *4*, 345–351.

Komarov, P.G., Komarova, E.A., Kondratov, R.V., Christov-Tselkov, K., Coon, J.S., Chernov, M.V., and Gudkov, A.V. (1999). A chemical inhibitor of p53 that protects mice from the side effects of cancer therapy. Science *285*, 1733–1737.

Komarova, E.A., Krivokrysenko, V., Wang, K., Neznanov, N., Chernov, M.V., Komarov, P.G., Brennan, M.L., Golovkina, T.V., Rokhlin, O.W., Kuprash, D.V., et al. (2005). p53 is a suppressor of inflammatory response in mice. FASEB J. *19*, 1030–1032.

Kwon, H.J., Won, Y.S., Suh, H.W., Jeon, J.H., Shao, Y., Yoon, S.R., Chung, J.W., Kim, T.D., Kim, H.M., Nam, K.H., et al. (2010). Vitamin D3 upregulated protein 1 suppresses TNF-α-induced NF-κB activation in hepatocarcinogenesis. J. Immunol. *185*, 3980–3989.

Kwon, H.J., Won, Y.S., Yoon, Y.D., Yoon, W.K., Nam, K.H., Choi, I.P., Kim, D.Y., and Kim, H.C. (2011). Vitamin D3 up-regulated protein 1 deficiency accelerates liver regeneration after partial hepatectomy in mice. J. Hepatol. *54*, 1168–1176.

Lee, K.N., Kang, H.S., Jeon, J.H., Kim, E.M., Yoon, S.R., Song, H., Lyu, C.Y., Piao, Z.H., Kim, S.U., Han, Y.H., et al. (2005). VDUP1 is required for the development of natural killer cells. Immunity *22*, 195–208.

Leung, K.M., Po, L.S., Tsang, F.C., Siu, W.Y., Lau, A., Ho, H.T., and Poon, R.Y. (2002). The candidate tumor suppressor ING1b can stabilize p53 by disrupting the regulation of p53 by MDM2. Cancer Res. *62*, 4890–4893.

Liu, X., Chua, C.C., Gao, J., Chen, Z., Landy, C.L., Hamdy, R., and Chua, B.H. (2004). Pifithrin-alpha protects against doxorubicin-induced apoptosis and acute cardiotoxicity in mice. Am. J. Physiol. Heart Circ. Physiol. *286*, H933–H939.

Liu, Z., Lu, H., Shi, H., Du, Y., Yu, J., Gu, S., Chen, X., Liu, K.J., and Hu, C.A. (2005). PUMA overexpression induces reactive oxygen species generation and proteasome-mediated stathmin degradation in colorectal cancer cells. Cancer Res. *65*, 1647–1654.

Liu, B., Chen, Y., and St Clair, D.K. (2008). ROS and p53: a versatile partnership. Free Radic. Biol. Med. *44*, 1529–1535.

Liu, Y., Elf, S.E., Miyata, Y., Sashida, G., Liu, Y., Huang, G., Di Giandomenico, S., Lee, J.M., Deblasio, A., Menendez, S., et al. (2009). p53 regulates hematopoietic stem cell quiescence. Cell Stem Cell *4*, 37–48.

Macip, S., Igarashi, M., Berggren, P., Yu, J., Lee, S.W., and Aaronson, S.A. (2003). Influence of induced reactive oxygen species in p53-mediated cell fate decisions. Mol. Cell. Biol. *23*, 8576–8585.

Matheu, A., Maraver, A., Klatt, P., Flores, I., Garcia-Cao, I., Borras, C., Flores, J.M., Viña, J., Blasco, M.A., and Serrano, M. (2007). Delayed ageing through damage protection by the Arf/p53 pathway. Nature *448*, 375–379.

Miyamoto, K., Araki, K.Y., Naka, K., Arai, F., Takubo, K., Yamazaki, S., Matsuoka, S., Miyamoto, T., Ito, K., Ohmura, M., et al. (2007). Foxo3a is essential for maintenance of the hematopoietic stem cell pool. Cell Stem Cell *1*, 101–112.

Naka, K., Muraguchi, T., Hoshii, T., and Hirao, A. (2008). Regulation of reactive oxygen species and genomic stability in hematopoietic stem cells. Antioxid. Redox Signal. *10*, 1883–1894.

Olovnikov, I.A., Kravchenko, J.E., and Chumakov, P.M. (2009). Homeostatic functions of the p53 tumor suppressor: regulation of energy metabolism and antioxidant defense. Semin. Cancer Biol. *19*, 32–41.

Patwari, P., Higgins, L.J., Chutkow, W.A., Yoshioka, J., and Lee, R.T. (2006). The interaction of thioredoxin with Txnip. Evidence for formation of a mixed disulfide by disulfide exchange. J. Biol. Chem. *281*, 21884–21891.

Rainwater, R., Parks, D., Anderson, M.E., Tegtmeyer, P., and Mann, K. (1995). Role of cysteine residues in regulation of p53 function. Mol. Cell. Biol. *15*, 3892–3903.

Sablina, A.A., Budanov, A.V., Ilyinskaya, G.V., Agapova, L.S., Kravchenko, J.E., and Chumakov, P.M. (2005). The antioxidant function of the p53 tumor suppressor. Nat. Med. *11*, 1306–1313.

Sasaki, M., Kawahara, K., Nishio, M., Mimori, K., Kogo, R., Hamada, K., Itoh, B., Wang, J., Komatsu, Y., Yang, Y.R., et al. (2011). Regulation of the MDM2-P53 pathway and tumor growth by PICT1 via nucleolar RPL11. Nat. Med. *17*, 944–951.

Schulze, P.C., De Keulenaer, G.W., Yoshioka, J., Kassik, K.A., and Lee, R.T. (2002). Vitamin D3-upregulated protein-1 (VDUP-1) regulates redox-dependent vascular smooth muscle cell proliferation through interaction with thioredoxin. Circ. Res. *91*, 689–695.

Shin, D., Jeon, J.H., Jeong, M., Suh, H.W., Kim, S., Kim, H.C., Moon, O.S., Kim, Y.S., Chung, J.W., Yoon, S.R., et al. (2008). VDUP1 mediates nuclear export of HIF1alpha via CRM1-dependent pathway. Biochim. Biophys. Acta *1783*, 838–848.

Sinha, K., Das, J., Pal, P.B., and Sil, P.C. (2013). Oxidative stress: the mitochondria-dependent and mitochondria-independent pathways of apoptosis. Arch. Toxicol. Published online March 30, 2013. http://dx.doi.org/10.1007/s00204-013-1034-4.

Sohn, D., Graupner, V., Neise, D., Essmann, F., Schulze-Osthoff, K., and Jänicke, R.U. (2009). Pifithrin-alpha protects against DNA damage-induced apoptosis downstream of mitochondria independent of p53. Cell Death Differ. *16*, 869–878.

Song, H., Cho, D., Jeon, J.H., Han, S.H., Hur, D.Y., Kim, Y.S., and Choi, I. (2003). Vitamin D(3) up-regulating protein 1 (VDUP1) antisense DNA regulates tumorigenicity and melanogenesis of murine melanoma cells via regulating the expression of fas ligand and reactive oxygen species. Immunol. Lett. *86*, 235–247.

Stambolsky, P., Weisz, L., Shats, I., Klein, Y., Goldfinger, N., Oren, M., and Rotter, V. (2006). Regulation of AIF expression by p53. Cell Death Differ. *13*, 2140–2149.

Sudo, K., Ema, H., Morita, Y., and Nakauchi, H. (2000). Age-associated characteristics of murine hematopoietic stem cells. J. Exp. Med. *192*, 1273–1280.

Vousden, K.H., and Lane, D.P. (2007). p53 in health and disease. Nat. Rev. Mol. Cell Biol. *8*, 275–283.

Zhou, R., Tardivel, A., Thorens, B., Choi, I., and Tschopp, J. (2010). Thioredoxin-interacting protein links oxidative stress to inflammasome activation. Nat. Immunol. *11*, 136–140.

Zhuo, X., Niu, X.H., Chen, Y.C., Xin, D.Q., Guo, Y.L., and Mao, Z.B. (2010). Vitamin D3 up-regulated protein 1(VDUP1) is regulated by FOXO3A and miR-17-5p at the transcriptional and post-transcriptional levels, respectively, in senescent fibroblasts. J. Biol. Chem. *285*, 31491–31501.